SETSCI Conference Indexing System,
Volume 3 (2018), 353-356

ISAS 2018-Winter
2nd International Symposium on Innovative Approaches in Scientific Studies
November 30 – December 2, 2018, Samsun, Turkey

Improving Hyperspectral Image Classification with Watershed Segmentation-Based Texture Features

Cigdem Serifoglu Yilmaz[1], Volkan Yilmaz[1*+] and Oguz Gungor[1]

[1]*Department of Geomatics, Karadeniz Technical University, Trabzon, Turkey*
[*]*Corresponding author: volkanyilmaz.jdz@gmail.com*
[+]*Speaker: volkanyilmaz.jdz@gmail.com*
Presentation/Paper Type: Oral

Abstract – Hyperspectral images offer a good separability among land cover classes, owing to their advantages to provide spectral bands with narrow wavelength intervals. It is also possible to further increase classification accuracy of hyperspectral images by integrating some auxiliary data to classification process. The aim of this study was to increase the classification accuracy of AVIRIS (Airborne Visible Infrared Imaging Spectrometer) and ROSIS (Reflective Optics System Imaging Spectrometer) hyperspectral data by integrating the Watershed Segmentation (WS)-based texture features to the SVM (Support Vector Machines) and RF (Random Forest) classification process. Since the used hyperspectral images contained a high number of bands, the PCA (Principal Component Analysis) technique was used to reduce the dimensionality of texture features and avoid redundant texture characteristics. It was found that the used procedure increased the RF classification accuracy of the AVIRIS and ROSIS data by 13.89% and 23.93%, respectively. It was also concluded that the SVM classification accuracy of the AVIRIS and ROSIS data was increased by 18.89% and 30.42%, respectively.

Keywords – *image classification, texture extraction, watershed segmentation, hyperspectral imagery*

I. Introduction

Hyperspectral sensors provide useful information about the features on the earth surface, owing to their ability to store the electromagnetic energy as multiple image bands (up to hundreds) with narrow wavelength intervals. This, of course, facilitates to distinguish between land cover classes. [1]-[8] are just some of the studies in which hyperspectral images were used for land cover mapping. Image classification is one of the most commonly-used land cover mapping techniques.

Image classification, which has always been one of the hottest topics of digital image processing applications, refers to the task of grouping image pixels into homogenous partitions with respect to their color characteristics. Image classification is not only used for land cover mapping [9], but also for applications such as point cloud filtering [10], diagnosing genetic syndrome [11], marine habitat mapping [12], mobile web browsing [13], fecal and ingesta identification [14], automatic color correction [15], object recognition [16], mobile robot navigation [17] etc.

Since image classification plays a significant role in the extraction of useful information from the surface of the earth, researchers have put so much effort either into developing new classification approaches or into improving the existing ones with extra procedures. Recently, classifiers like Minimum Distance and Parallelpiped can be considered below the state-of-the-art, compared to advanced algorithms like the RF, SVM, Artificial Neural Network etc. It is even possible to further increase the performance of the classification algorithms by incorporating texture feature information into classification process [18], [19]. The aim of this study was to improve the performances of the SVM and RF classification algorithms on hyperspectral images by integrating the texture features extracted from WS-based image segments.

A. Image Classification

The SVM algorithm, developed by Vapnik [20], was originally developed to distinguish two linearly-separable classes [21]. It aims at finding the optimum hyperplane maximizing the margin between classes [22]. If classes are linearly-separable, then the SVM algorithm places the optimum hyperplane in the middle of the two parallel planes maximizing the margin between classes [20]. However, classes cannot be separated linearly in most real-world applications. In such cases, the SVM algorithm uses a nonlinear function to project the data onto a higher-dimensional space on which the classes can be separated easier [22]. Many real-world applications require the separation of more than two classes, which motivated researchers to develop multi-class approaches for this problem such as the One-Against-One [23], One-Against-All [24] and hierarchical tree-based strategies [25]. Further information about the SVM classifier can be found in [20], [22], [25] and [26].

The RF classification algorithm employs classifiers (trees) generated from vectors that are sampled randomly and independently. Classifiers are generated from the training sets in input vectors. Each tree gives a vote for the most popular class and input vector is classified [27]. The RF algorithm defines the class with the most votes. A RF is generated with respect to some bagging and random subspace techniques. Bagging is used to increase the RF classification accuracy [28]. Let N be the size of the training set, the bagging technique generates new n-dimensional ($n < N$) data sets. Considering the data includes M features, m ($m < M$) features are selected randomly for each tree node in order to calculate the best separability within that node. Once the RF is generated, each sample is assigned to the class that received the most votes from the trees [22].

B. Watershed Segmentation

The WS, developed for image segmentation by Digabel and Lantuéjoul [29] and improved in [30], is a morphological-based algorithm that considers every image as a topographical relief [31]. The WS is applied to the image gradient. The aim of the WS is to find segments of high intensity gradients dividing neighbouring local minima (basins) [32].

Consider a topographical relief is immersed into a lake. As the relief goes down, the catchment basins will tend to fill up with water starting from the local minima of the relief. The WS algorithm builds infinitely tall dams (watershed lines) where the water in catchment basins starts to merge. All watershed lines generated on the relief gives the WS result [31]. The WS algorithm tends to lead to oversegmentation due to the fact that it is very sensitive to small magnitude variations in images [33]. Oversegmentation problem is tackled by using region merging techniques [34], employing markers [35] or examining the evolution of the catchment basins in Gaussian scale-space [33], [36].

C. Texture Feature Computation

The range, mean, variance and entropy texture features were computed in this study to increase the classification performances of the SVM and RF classifiers. These features were given in [37] as;

$$Range\ (R) = g_{max} - g_{min} \tag{1}$$

$$Mean\ (M) = \sum_{i=0}^{N_g-1} i\ P(i) \tag{2}$$

$$Variance\ (V) = \sum_{i=0}^{N_g-1} (i-M)^2\ P(i) \tag{3}$$

$$Entropy\ (E) = -\sum_{i=0}^{N_g-1} P(i) * \ln P(i) \tag{4}$$

where, g_{max} and g_{min} stand for the maximum and minimum values in sliding kernel, respectively. N_g defines the number of distinct grey levels within the quantized image and $P(i)$ denotes the probability of each pixel value [37], [38].

II. Application

A. Test Sites and Data

The first test data 'Indian Pines' [39], which has 220 spectral bands of dimension 145×145, was gathered by the AVIRIS sensor over the north-western Indiana in 1992. The data has a spatial resolution of 20 m. Two-thirds of the scene includes agricultural products, whereas one-third of the scene consists of forest and other vegetation. The ground truth data includes sixteen classes [40]. In this study, seven classes with smaller number of samples were ignored. Nine classes of corn-no till, corn-min till, grass-pasture, grass-trees, hay-windowed, soybean-no till, soybean-min till, soybean-clean and woods were considered in the study. Prior to processing, the water absorption bands, which were in the ranges of 104-108 and 150-163, were removed to avoid their negative influences on classification results.

The second test data 'Pavia University', which was acquired by the ROSIS sensor over Pavia, northern Italy, includes 103 spectral bands of dimension 610×340. The data has a spatial resolution of 1.3 m. The reference data includes nine classes of asphalt, meadows, gravel, trees, painted metal sheets, bare soil, bitumen, self-blocking bricks and shadows. All classes were considered in this study. The Indian Pines and Pavia University datasets are shown in Figure 1.

Indian Pines Pavia University

Fig. 1 Test sites

B. Methodology

As a first step, the WS algorithm was applied on both data sets. Afterwards, the range, mean, variance and entropy texture features were calculated from the image segments. This process led to four texture features for each spectral band, which resulted in a total of 804 and 412 texture bands for the Indian Pines and Pavia University data, respectively. Since there were an excessive number of texture bands, a feature reduction method was needed to reduce the texture data by eliminating redundant texture information. Hence, the PCA was applied on the range, mean, variance and entropy texture feature groups separately to find the optimum texture characteristics representing the whole texture features. A number of combinations of the PCA-derived texture features were combined with the original hyperspectral data sets to increase the classification accuracies of the SVM and RF classifiers as much as possible. The RF algorithm used 100 trees to classify the imageries. The gamma and penalty parameters of the SVM algorithm were set to 1 and 100, respectively. Also, radial basis function was used as the kernel type of the SVM classification algorithm.

III. Results

Table 1 shows the classification accuracies of the images obtained by combining the original hyperspectral images (HS) and combinations of the PCA-derived texture features. As seen in Table 1, integrating the PCA-derived texture features into the SVM and RF procedures increased the classification performances in almost all cases.

Table 1 shows that combining the 3 PCs of the range, mean, variance and entropy texture bands (HS + 12 Texture PCs) with the original HS imagery increased the RF classification accuracy of the Indian Pines and Pavia University data from 64.65% to 69.40% and from 78.66% to 97.48%, respectively. Same procedure slightly decreased the SVM classification accuracy of the Indian Pines data (from 63.64% to 63.51%),

and increased the SVM accuracy of the Pavia University from 74.89% to 94.20%.

Table 1 also reveals the fact that classification performances of the RF and SVM algorithms tended to increase as did the number of PCs. However, integrating more than 40 PCs for each texture feature group caused significant decreases in the classification accuracy, which was why classification accuracies of the images with up to 40 PCs for each texture feature group were given in Table 1.

As seen in Table 1, for the Indian Pines data set, the best RF and SVM classification performances were achieved by integrating 30 (HS + 120 Texture PCs) and 35 (HS + 140 Texture PCs) texture PCs for each texture feature group, respectively. On the other hand, for Pavia University data set, the best RF and SVM classification performances were obtained by integrating 35 (HS + 140 Texture PCs) and 40 (HS + 160 Texture PCs) texture PCs for each texture feature group, respectively.

Table 1. RF and SVM classification accuracies computed for the data sets

Data set	RF (%)		SVM (%)	
	Indian Pines	Pavia Uni.	Indian Pines	Pavia Uni.
HS	64.65	78.66	63.64	74.89
HS + 12 Texture PCs	69.40	**97.48**	63.51	94.20
HS + 20 Texture PCs	70.98	97.23	66.58	95.05
HS + 40 Texture PCs	70.79	97.14	65.63	97.14
HS + 60 Texture PCs	71.99	96.96	65.12	97.38
HS + 80 Texture PCs	70.72	96.38	71.92	97.59
HS + 100 Texture PCs	73.06	96.70	73.60	97.64
HS + 120 Texture PCs	**73.63**	96.93	74.71	97.60
HS + 140 Texture PCs	73.47	97.33	**75.66**	97.64
HS + 160 Texture PCs	71.26	96.15	73.57	**97.67**

Figures 2 and 3 present the classification results of the original HS images and of the datasets provided the greatest classification accuracy increase.

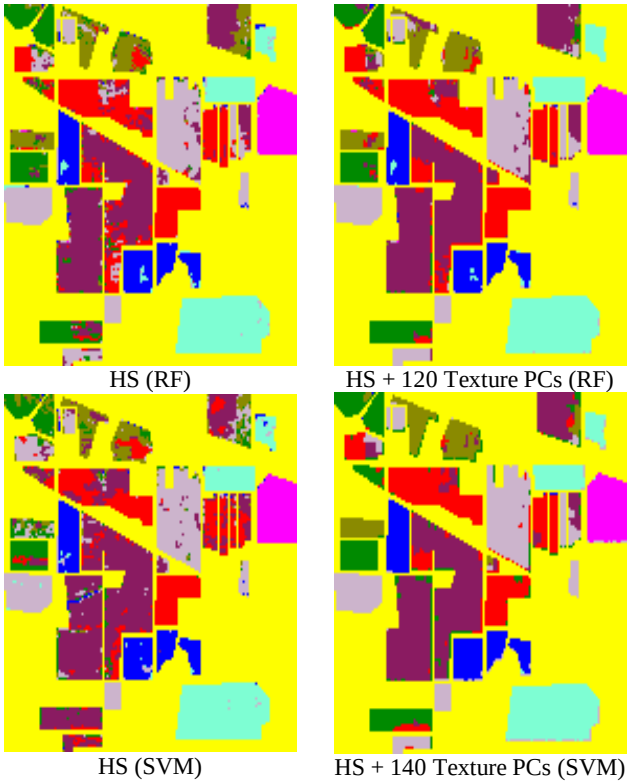

Fig. 2 Classification results for the Indian Pines dataset

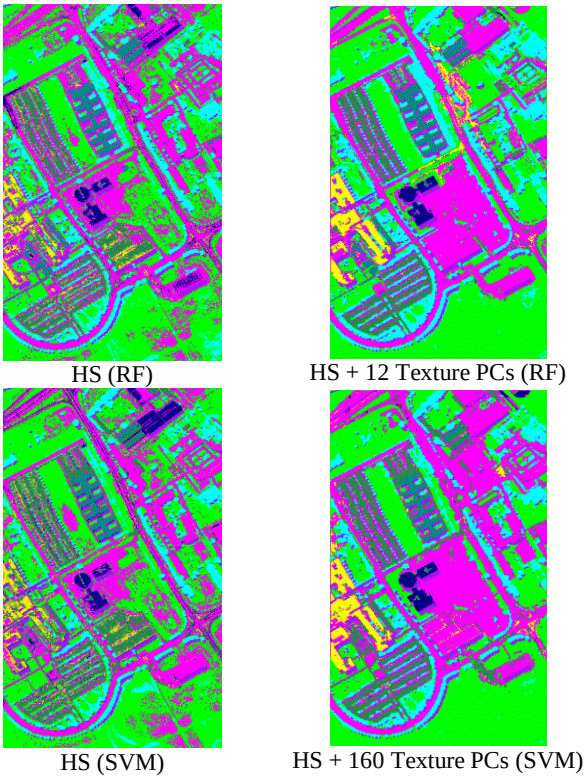

Fig. 3 Classification results for the Pavia University dataset

IV. Conclusion

This study aimed at improving the hyperspectral image classification performances of the RF and SVM classifiers by integrating the WS-based texture features into the classification procedures. Experiments revealed that the RF classification accuracy of the Indian Pines and Pavia University data was increased by 13.89% and 23.93%, respectively. On the other hand, the SVM classification accuracy of the Indian Pines and Pavia University data was increased by 18.89% and 30.42%, respectively. Integrating different combinations of the texture PCs into the classification procedures may further improve the classification accuracies.

Acknowledgment

We would like to thank Prof. Paola Gamba from the Telecommunications and Remote Sensing Laboratory, Pavia University (Italy) for providing the Pavia University data and Prof. David Landgrebe from Purdue University (USA) for providing the Indian Pines data.

References

[1] F. Tsai, and W. D. Philpot, "A derivative-aided hyperspectral image analysis system for land-cover classification," *IEEE T. Geosci. Remote Sens.*, vol. 40, no. 2, pp. 416-425, 2002.

[2] A. Hirano, M. Madden, and R. Welch, "Hyperspectral image data for mapping wetland vegetation," *Wetlands*, vol. 23 no. 2, pp. 436-448, 2003.

[3] J. F. Knight, R. S. Lunetta, J. Ediriwickrema, and S. Khorram, "Regional scale land cover characterization using MODIS-NDVI 250 m multi-temporal imagery: A phenology-based approach," *GISci. Remote Sens.*, vol. 43, no. 1, pp. 1-23, 2006.

[4] B. Xu, and P. Gong, "Land-use/land-cover classification with multispectral and hyperspectral EO-1 data," *Photogramm. Eng. Remote Sens.*, vol. 73, no. 8, pp. 955-965, 2007.

[5] J. C. W. Chan, and D. Paelinckx, "Evaluation of Random Forest and Adaboost tree-based ensemble classification and spectral band

selection for ecotope mapping using airborne hyperspectral imagery," *Remote Sens. Environ.*, vol. 112, no. 6, pp. 2999-3011, 2008.

[6] R. Duca, and F. Del Frate, "Hyperspectral and multiangle CHRIS–PROBA images for the generation of land cover maps," *IEEE T. Geosci. Remote Sens*, vol. 46, no. 10, pp. 2857-2866, 2008.

[7] G. P. Petropoulos, K. Arvanitis, and N. "Sigrimis, Hyperion hyperspectral imagery analysis combined with machine learning classifiers for land use/cover mapping," *Expert Syst. Appl.*, vol. 39, no. 3, pp. 3800-3809, 2012.

[8] G. P. Petropoulos, C. Kalaitzidis, and K. P. Vadrevu, "Support vector machines and object-based classification for obtaining land-use/cover cartography from Hyperion hyperspectral imagery," *Comput. Geosci.*, vol. 41, pp. 99-107, 2012.

[9] I. Kanellopoulos, G. G. Wilkinson, and J. Megier, "Integration of neural network and statistical image classification for land cover mapping," In: *Geoscience and Remote Sensing Symposium (IGARSS'93)*, 1993, pp. 511-513.

[10] V. Yilmaz, B. Konakoglu, C. Serifoglu, O. Gungor, and E. Gökalp, "Image classification-based ground filtering of point clouds extracted from UAV-based aerial photos," *Geocarto Int.*, vol. 33, no. 3, pp. 310-320, 2018.

[11] A. David, and B. Lerner, "Support vector machine-based image classification for genetic syndrome diagnosis," *Pattern Recognit. Lett.*, vol. 26, no. 8, pp. 1029-1038, 2005.

[12] M. Lauer, and S. Aswani, "Integrating indigenous ecological knowledge and multi-spectral image classification for marine habitat mapping in Oceania," *Ocean Coast. Manage.*, vol. 51, no. 6, pp. 495-504, 2008.

[13] T. Maekawa, T. Hara, and S. Nishio, "Image classification for mobile web browsing," in: *Proc. 15th International Conference on World Wide Web*, 2006, pp. 43-52.

[14] B. Park, W. R. Windham, K. C. Lawrence, and D. P. Smith, "Hyperspectral image classification for fecal and ingesta identification by spectral angle mapper," in: *ASAE Annual Meeting, American Society of Agricultural and Biological Engineers*, 2004.

[15] C. Fredembach, M. Schröder, and S. Süsstrunk, "Region-based image classification for automatic color correction," in: *Color and Imaging Conference*, 2003, no. 1, pp. 59-65.

[16] J. Böhm, and C. Brenner, "Curvature-based range image classification for object recognition," in: *Intelligent Robots and Computer Vision XIX: Algorithms, Techniques, and Active Vision*, 2000, vol. 4197, pp. 211-221.

[17] Q. Zhou, K. Yuan, H. Wang, and H. Hu, "Fpga-based colour image classification for mobile robot navigation," in: *IEEE International Conference on Industrial Technology*, 2005, pp. 921-925.

[18] C. D. Lloyd, S. Berberoglu, P. J. Curran, and P. M. Atkinson, "A comparison of texture measures for the per-field classification of Mediterranean land cover," *Int. J. Remote Sens.*, vol. 25, no. 19, pp. 3943-3965, 2004.

[19] C. Serifoglu Yilmaz, E. Tunc Gormuş, and O. Gungor, "Texture Based Classification of Hyperspectral Images with Support Vector Machines Classifier" in: *International Symposium on GIS Applications in Geography & Geosciences (ISGGG)*, 2017.

[20] V. N. Vapnik, *The Nature of Statistical Learning Theory*, 1995.

[21] Y. C. Ouyang, H. M. Chen, J. W. Chai, C. C. Chen, C. C. C. Chen, S. K. Poon, C. W. Yang, and S. K. Lee, "Independent component analysis for magnetic resonance image analysis," *EURASIP J. Adv. Signal Process.*, 2008.

[22] A. Tso, and P. M. Mather, *Classification Methods for Remotely Sensed Data*, 2009.

[23] S. Knerr, L. Personnaz, and G. Dreyfus, "Single-layer learning revisited: a stepwise procedure for building and training a neural network," in: *Neurocomputing*, 1990, pp. 41-50.

[24] Y. Liu, and Y. F. Zheng, "One-against-all multi-class SVM classification using reliability measures," *Neural Netw.*, vol. 2, pp. 849-854, 2005.

[25] F. Melgani, and L. Bruzzone, "Classification of hyperspectral remote sensing images with support vector machines," *IEEE T. Geosci. Remote Sens.*, vol. 42, no. 8, pp. 1778-1790, 2004.

[26] M. Pal, "Ensemble of support vector machines for land cover classification," *Int. J. Remote Sens.*, vol. 29, no. 10, pp. 3043-3049, 2008.

[27] L. Breiman, "Random forests," *Machine Learning*, vol. 45, no. 1, pp. 5-32, 2001.

[28] L. Breiman, "Bagging predictors," *Machine Learning*, vol. 24, no. 2, pp. 123-140, 1996.

[29] H. Digabel, and C. Lantuéjoul, "Iterative algorithms," in: *Proc. 2nd European Symposium on Quantitavive Analysis of Microstructures in Material Sciences, Biology and Medecine*, pp. 39-49, 1977.

[30] H. Li, A. Elmoataz, J. M. Fadili, and S. Ruan, "An improved image segmentation approach based on level set and mathematical morphology," *in: 3rd International Symposium on Multispectral Image Processing and Pattern Recognition*, vol. 5286, pp. 851-855, 2003.

[31] M. S. H. Khiyal, A. Khan, and A. Bibi, "Modified Watershed Algorithm for Segmentation of 2D Images," *Issues in Informing Science & Information Technology*, 2009.

[32] N. Salman, Image segmentation based on watershed and edge detection techniques, *Int. Arab. J. Inf. Techn.*, vol. 3, no. 2, pp. 104-110, 2006.

[33] K. Karantzalos, and D. Argialas, "Improving edge detection and watershed segmentation with anisotropic diffusion and morphological levellings," *Int. J. Remote Sens.*, vol. 27, no. 24, pp. 5427-5434, 2006.

[34] K. Haris, S. N. Efstratiadis, N. Maglaveras, and A. K. Katsaggelos, "Hybrid image segmentation using watersheds and fast region merging," *IEEE T. Image Process.*, vol. 7, no. 12, pp. 1684-1699, 1998.

[35] F. Meyer, and P. Maragos, "Multiscale morphological segmentations based on watershed, flooding, and eikonal PDE," in: *International Conference on Scale-Space Theories in Computer Vision*, 1999, pp. 351-362.

[36] J. M. Gauch, Image segmentation and analysis via multiscale gradient watershed hierarchies, *IEEE T. Image Process.*, vol. 8, no. 1, pp. 69-79, 1999.

[37] H. Anys, A. Bannari, D. C. He, and D. Morin, "Texture analysis for the mapping of urban areas using airborne MEIS-II images," in: Proc. 1st International Airborne Remote Sensing Conference and Exhibition, 1994, vol. 3, pp. 231-245.

[38] *Harris Geospatial Solutions*, online help documentary.

[39] M. F. Baumgardner, L. L. Biehl, and D. A. Landgrebe, "220 band aviris hyperspectral image data set: June 12, 1992 indian pine test site 3," Purdue University Research Repository, 2015.

[40] (2018) Datasets for Classification. [Online]. Available: http://lesun.weebly.com/hyperspectral-data-set.html